A Chebyshev Transformer Based Microstrip to Groove Gap Waveguide Inline Transition for MMIC Packaging

José M. Pérez-Escudero, Alicia E. Torres-García, Ramón Gonzalo, *Member, IEEE,* and Iñigo Ederra, *Member, IEEE*

***Abstract*—Gap waveguide technology has become an alternative for millimetre and sub-millimetre wave electronic circuit packaging thanks to the loss reduction associated to its use. In this paper a simplified design of an inline transition between microstrip and groove gap waveguide operating at W-band is presented. The transition consists of a tapered microstrip line and a Chebyshev adapter that couple the quasi-TEM mode of the microstrip line to the so-called vertical mode of the groove gap waveguide. The simplicity of this design makes this transition appropriate for MMIC packaging at millimetre frequencies and above. The simulation results have been experimentally validated in the W-band. Good performance has been achieved: return loss better than 10 dB and mean insertion loss lower than 2 dB.**

***Index Terms*—Groove Gap Waveguide, Microstrip, Chebyshev Transformer, Waveguide Transition.**

I. Introduction

The number of applications at millimetre, sub-millimetre and terahertz frequencies is constantly growing. In the communications field, due to the saturation of the spectrum at low frequencies and the increasing demand for bandwidth in point-to-point wireless links, occupation of higher frequency bands becomes a good alternative for wireless backhaul, the next generation wireless 5G and wireless HDMI [**?**]. Moreover, high performance sensors at W-Band can be used for automotive radar [**?**]. In addition, the high resolution of mm-waves, their penetration through some materials (e.g. clothes, wood...), and the fact that, on the contrary to X-rays, they are not a threat for human health, allow their use for security imaging, e.g. for concealed weapon detection in airports [**?**].

The development of these applications requires efficient packaging solutions which allow integration of microstrip and waveguide based components. Packaging is important to protect the circuit not only from environmental hazards but also from mechanical stress that components may suffer. In addition, RF packaging allows isolating the circuits from external interferences. However, standard enclosings are liable to create resonant cavities if not properly controlled, which produces additional losses [**?**].

Recently, a novel approach for packaging has been proposed, based on the so-called bed of nails [**?**]. These are periodic metallic structures which avoid propagation of electromagnetic waves in a certain frequency range. Thanks to this property they have found its application for parasitic mode suppression [**?**]-[**?**]. In addition, pin surfaces allow creating waveguides if a linear defect is introduced [**?**]-[**?**]. These structures resemble metallic rectangular or ridge waveguides and a family of components are being developed based on them [**?**]-[**?**].

However, integration of MMIC components in these novel waveguide solutions requires transitions between them and planar technology transmission lines, such as microstrip or coplanar waveguide. Several of the proposed solutions are based on inline configurations. However, they require full-wave optimization, since they either rely on complex geometries [**?**]-[**?**] or are meant for low frequency operation [**?**].

In this paper, out of the several bed of nails based waveguide implementations [**?**], we will focus on the so-called Groove Gap Waveguide (GGW). This waveguide consists of an air channel in between two bed of nails sections. A simple alternative for an inline transition between this waveguide and microstrip working at W-Band will be presented. The transition design follows an analytical approach, similar to that in [**?**] and [**?**] but adjusting the design to the GGW propagation characteristics. As a consequence, since the dimensions are computed by means of the standard Chebyshev transformer design formulae, full wave optimization is avoided.

The structure of the paper is organized as follows. First, Section **??** describes the proposed transition, the analytic method for the design and the full wave simulation results. Afterwards, the manufacturing procedure and the experimental validation are presented in Section **??**. Finally, conclusions are drawn in Section **??**.

II. Transition Design and Simulation Results

The proposed inline transition is presented in Fig. **??**. The transition consists of two sections: a linear transition from microstrip to dielectric filled GGW and a Chebyshev transformer from dielectric filled GGW to standard (air filled) GGW. The operating principle is based on the high similitude between the field distribution of the so-called vertical mode of the GGW [**?**] and the rectangular waveguide TE_{10} mode. This allows employing a technique for the design of this transition similar to that used in [**?**]. Even though this principle and the design procedure presented for this kind of transition is

The authors are with the Department of Electrical, Electronic and Communication Engineering, Public University of Navarra, Spain, 31006 and with the Institute of Smart Cities, Public University of Navarra, Spain, 31006
E-mail: josemanuel.perez@unavarra.es, aliciaelena.torres@unavarra.es, inigo.ederra@unavarra.es and ramon@unavarra.es.

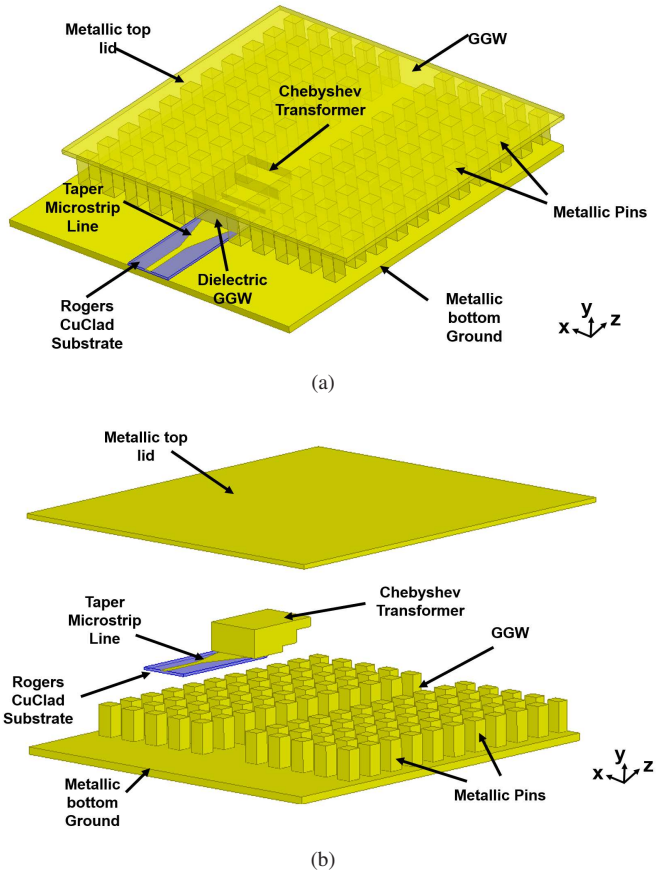

Fig. 1: (a)Perspective view the proposed microstrip to groove gap waveguide (GGW) transition. (b) Explosion view of the microstrip to GGW transition. Note that the Chebyshev transformer is not an independent piece.

TABLE I: Dimensions of the unit cell of the bed of nails, see Fig. **??**.

Parameter	Description	Value (μm)
d	Pin height	1190
a	Pin size	600
h	Air gap	80
p	Period	1240

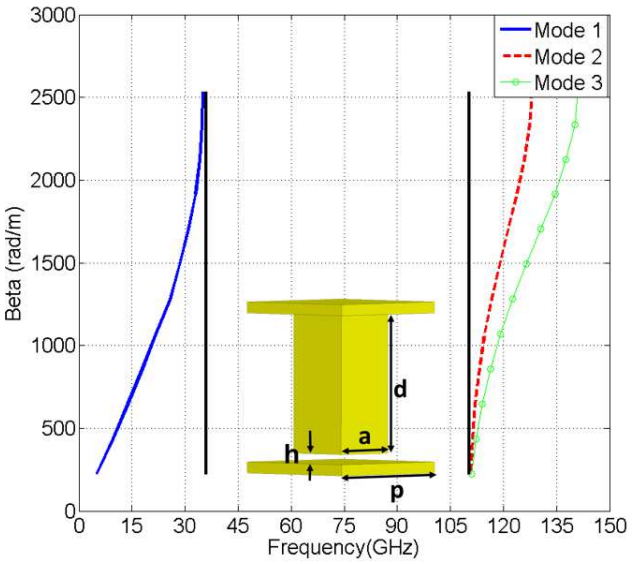

Fig. 2: Dispersion diagram of the periodic unit cell. The vertical lines represent the limits of the band-gap.

applicable to any frequency band, in this case the transition will be realized to work at W-Band.

A. Groove Gap Waveguide Design

The GGW consists of an air channel in between two periodic metallic pin sections. This periodic metallic pin distribution that surrounds the waveguide, also referred to as bed of nails, is designed to have its band-gap in the desired frequency range [**?**], [**?**]. In this case, the pin parameters were optimized so that the band-gap covers from 50 GHz to 110 GHz, which includes the W-band, and the final dimensions are gathered in Table **??**. The resulting dispersion diagram, computed with Ansys HFSS eigenmode solver, is shown in Fig. **??**, where we can observe that the band-gap, determined by the highest frequency of the first mode of the dispersion diagram and the lowest frequency of the second mode of the dispersion diagram, covers the full W-band.

Based on this pin structure a GGW was created by leaving an air channel in between them. This creates a propagation band in the band-gap of the periodic structure. In order to make the resulting GGW compatible with a W-band WR10 rectangular waveguide, the height of the GGW will be the same as that of the WR10 waveguide, i.e. 1.27 mm. Regarding the width, w in the inset in Fig. **??**, it will be adjusted for monomode operation in the desired frequency range. In our case, in order to facilitate testing, it should also provide good matching to a WR10 waveguide. The best result was obtained for $w = 2.45$ mm and the performance of this direct connection is shown in Fig. **??**. The return loss is higher than 25 dB within the W-band operational bandwidth (75-110 GHz) and the insertion loss is negligible, below 0.1 dB. The different width between GGW and standard waveguide is caused by the different boundary condition at the waveguide walls, which allow evanescent fields to penetrate the lateral pin regions. In this case five periods of pins surround the waveguide. Even though a smaller number of pins would be enough to prevent leakage, the whole available area was covered with pins.

B. Transition design

As mentioned, the transition is divided into two parts: a microstrip linear taper and a Chebyshev transformer between dielectric filled and air filled GGW (see Fig. **??** for details).

The first part corresponds to a microstrip linear taper, whose top view is shown in Fig. **????**. This line, which matches the 50 Ω microstrip line to the dielectric filled GGW (DFGGW) impedance, is calculated using the standard microstrip impedance formulae and a $3\lambda_g/4$ length [**?**]. It is printed on 100 μm thick Rogers CuClad 233 (ϵ_r = 2.34 and $\tan\delta$ = 0.009) where the required width to obtain the 50 Ω characteristic impedance is 300 μm.

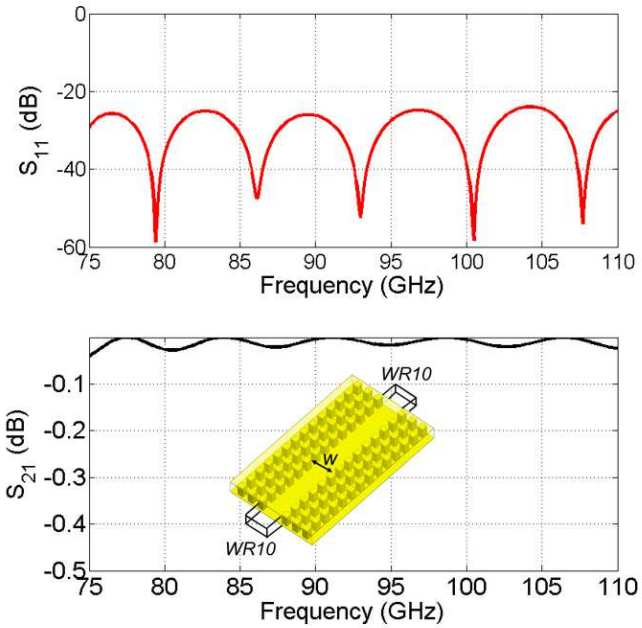

Fig. 3: Performance of a direct connection between a groove gap waveguide and a WR-10 rectangular waveguide.

The second part of the transition follows a similar approach to that proposed in [**?**]. The impedances of the Chebyshev transformer sections are calculated by the standard formulation [**?**].

First, the order of the transition necessary to satisfy the maximum value of reflection coefficient, A, is calculated as:

$$A = \log\left(\frac{R_L}{Z_0}\right)\frac{1}{2T_N(\sec\theta_M)} \tag{1}$$

where T_N is Chebyshev polynomial of order N, N is the order of the Chebyshev transformer, R_L is the load impedance (in this case the impedance of the air filled GGW), Z_0 is the input impedance (in this case, the dielectric filled GGW).

The parameter θ_M is given by:

$$\theta_M = \frac{\pi}{2}(1 - \frac{\Delta f}{2f_0}) \tag{2}$$

where Δf is the transformer bandwidth and f_0 is the central frequency.

The impedance of the different waveguide sections are calculated as the waveguide electric impedance [**?**].

$$Z_{wg} = 2\frac{\eta_0}{\sqrt{\epsilon_r}}\frac{b}{w} \tag{3}$$

where η_0 is the vacuum impedance, ϵ_r is the dielectric constant of the GGW filling medium (the microstrip dielectric substrate for the DFGW and air for the rest of them), b is the height of the GGW section and w is the width of the GGW, 2.45 mm.

The reflection coefficients are calculated by equating the terms.

$$\begin{aligned}\rho(\theta) = 2e^{-jN\theta}[\rho_0 cosN\theta + \rho_1 cos(N-2)\theta + \ldots + \\ \rho_n cos(N-2n)\theta + \ldots] = Ae^{(-jN\theta)}T_N(sec\theta_m cos\theta)\end{aligned} \tag{4}$$

For this design a three section transformer is enough to obtain return loss higher than 15 dB in the full W-band and these values are calculated as

$$\rho_0 = \frac{A\sec^3\theta_M}{2} \tag{5}$$

$$\rho_1 = \frac{3A(\sec^3\theta_M - \sec\theta_M)}{2} \tag{6}$$

and $\rho_2 = \rho_1$ because of the symmetry of the Chebyshev transformer. Finally, the impedance of the n-th section, Z_n, is obtained as:

$$Z_n = Z_{n-1}e^{2\rho_{n-1}} \tag{7}$$

These impedances correspond to the electric impedance of a waveguide and their heights are calculated from (**??**):

$$b_n = w\frac{Z_{wg,n}}{2}\frac{\sqrt{\epsilon_r}}{\eta_0} \tag{8}$$

where $Z_{wg,n}$ is the impedance of the n-th GGW section.

Fig. **????** shows a perspective view of the three steps of the half-split Chebyshev transformer with waveguide height b_n and length l_n, which corresponds to $\lambda_g/4$. The input GGW section is filled with dielectric, and its height corresponds to the substrate thickness plus the metal cladding. Note that there is no restriction on its length, since this section is not strictly a part of the Chebyshev transformer. The same value as for the other sections has been taken. In addition, given the change of dielectric, the required impedance of the first section is obtained with the same height, i.e. $b_1 = b_0$.

The dimensions of the whole transition can be seen in Table **??**. The structure has been simulated using the commercial Finite Element Method solver Ansys HFSS. First, the two different parts, i.e. the microstrip to dielectric filled GGW and the Chebyshev transformer between dielectric filled GGW and air filled GGW, have been simulated separately. These results are presented in Fig. **??**. It can be seen that the return loss is better than 20 dB for both cases. On the other hand, the insertion loss are lower than 0.5 dB for both cases. Nonetheless, in the microstrip case the losses are higher, due to the dielectric and radiation losses. Note that these results have been obtained with the analytic procedure above, without any full-wave optimization.

The back-to-back transition includes a 5.18 mm microstrip line in between the two transitions; the model used for simulation is shown in Fig. **??**. When the whole transition is analysed, the insertion and return loss results shown in Fig. **??** are obtained. In this figure, the microstrip to GGW single and back-to-back transitions are compared.

The mean insertion loss is 0.66 dB for the single transition and 1 dB for the back-to-back configuration. The higher insertion loss in the back-to-back configuration is ascribed to the substrate losses in the longer microstrip line. The losses in the microstrip line have been calculated by full wave simulation in HFSS taking into account the loss tangent of the dielectric material at high frequencies ($tan\delta = 0.009$). For the single transition these losses are 0.33 dB. Therefore, the losses of the transition can be estimated as $0.66 - 0.33 = 0.33$ dB. The mean return loss is 24.1 dB and 17.2 dB for the single and back-to-back transitions, respectively. The back-to-back

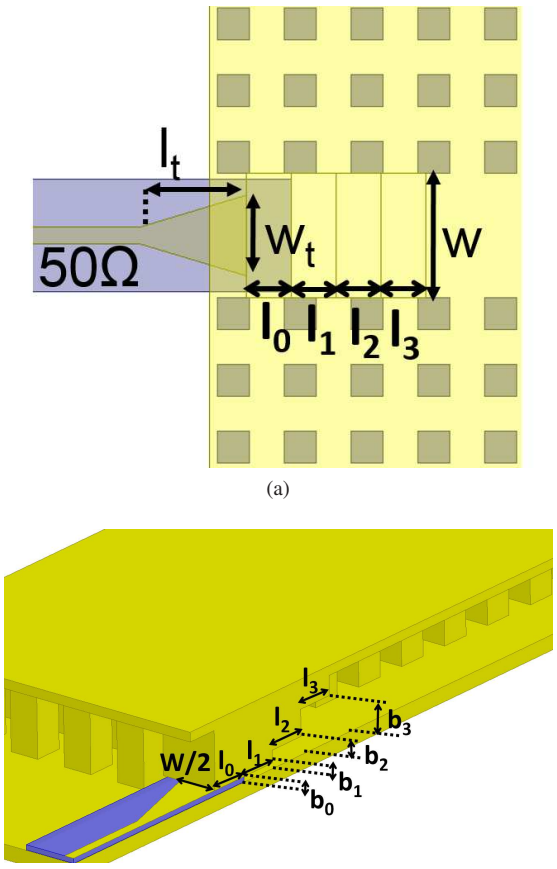

Fig. 4: Microstrip to groove gap waveguide transition: (a)Top View and (b) Perspective view of the half-split transition.

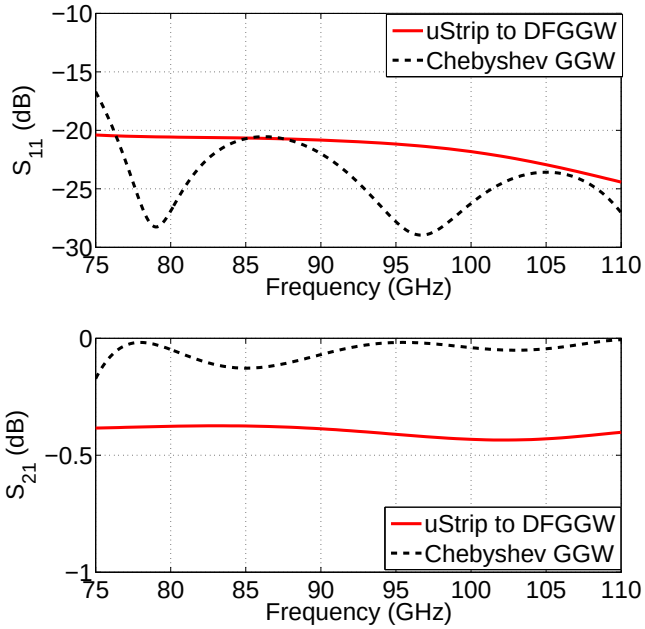

Fig. 5: Simulation of the scattering parameters of the microstrip to dielectric filled GGW (solid line) and the GGW Chebyshev transformer (dashed line).

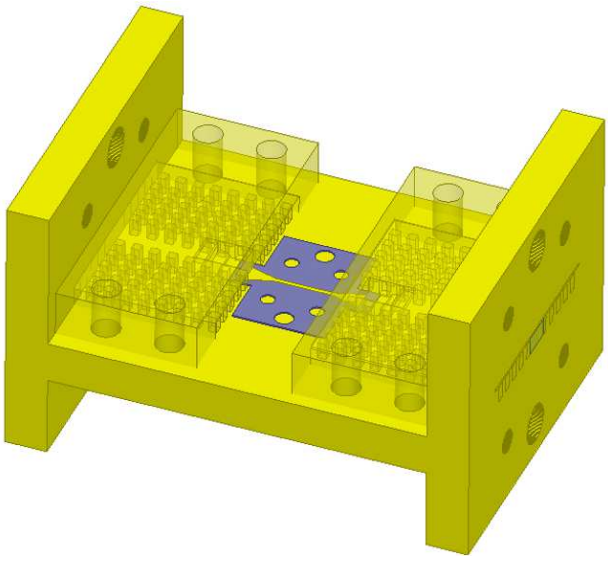

Fig. 6: 3D perspective view of the back-to-back transition model used for HFSS simulation.

TABLE II: Dimensions of the transition (μm).

Parameter	Description	Design	Fabricated
l_t	Microstrip taper length	1500	1467
w_t	Microstrip taper width	1300	1256
b_0	Input GGW height	116	158
b_1	GGW Section 1 height	116	158
b_2	GGW Section 2 height	380	407
b_3	GGW Section 3 height	950	953
l_0	Input GGW length	830	859
l_1	GGW Section 1 length	830	821
l_2	GGW Section 2 length	830	810
l_3	GGW Section 3 length	830	810
w	GGW width	2450	2290
b	WR-10 waveguide height	1270	1280

transition presents worse S_{11} due to the non perfect matching at both ports. Anyway, return loss is better than 15 dB for almost the whole band in both configurations. In Fig. **??** the electric field distribution at 92.5 GHz is shown. It can be observed that the Quasi-TEM mode of the microstrip line couples to the vertical mode of the GGW. Furthermore, the mode confinement in the GGW region thanks to the bed of nails can be also appreciated, although the field evanescently decays in the pin areas.

C. Tolerance analysis

The effect of different manufacturing and assembly errors will be evaluated in this section. First, the effect of the air gap between the bed of nails and the lid on the performance of the transition will be studied. As a matter of fact, one of the main problems when rectangular waveguides are split in the H-Plane is the tight contact required between both parts in order to reduce losses. This problem is alleviated by the use of the bed of nails, since no contact is required. In our design an 80 μm air gap has been considered at the end of the pins. To evaluate the error tolerance on this air gap the pin length has been swept around the nominal value. The results are shown in Fig. **??**. We can observe that when the air gap is

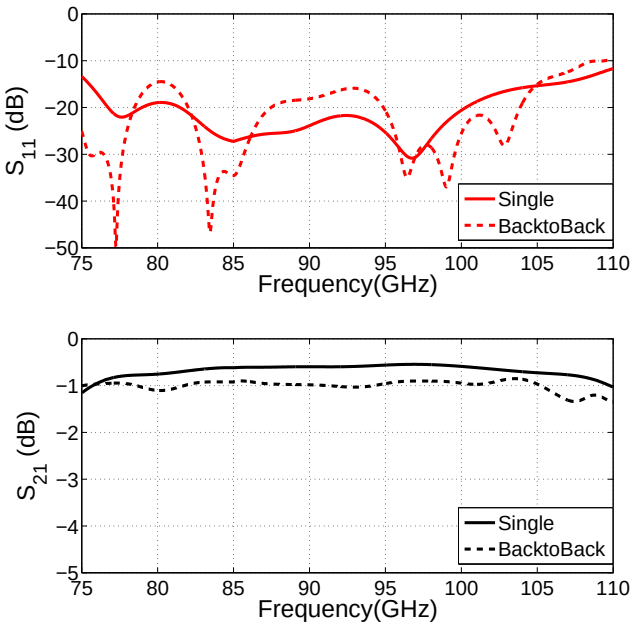

Fig. 7: Simulation of the scattering parameters for the microstrip to groove gap waveguide single (solid line) and back-to-back transitions (dashed line).

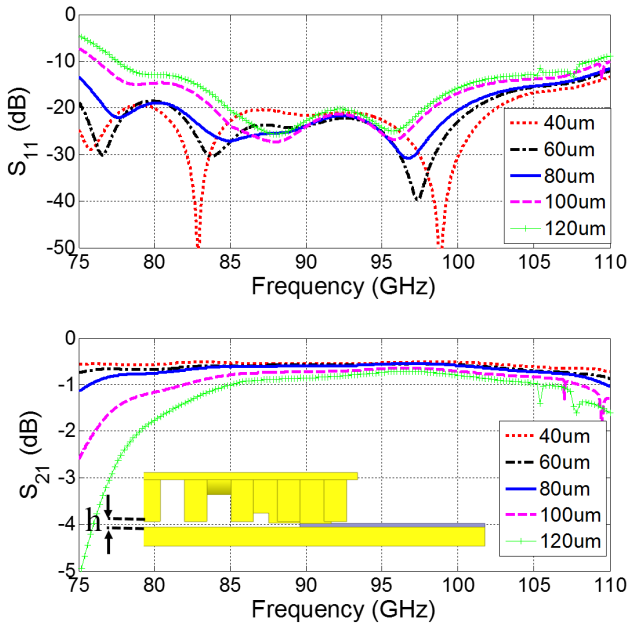

Fig. 9: Evaluation of the effect on the transition performance of errors in the fabrication of the metallic pins, given by different values of h.

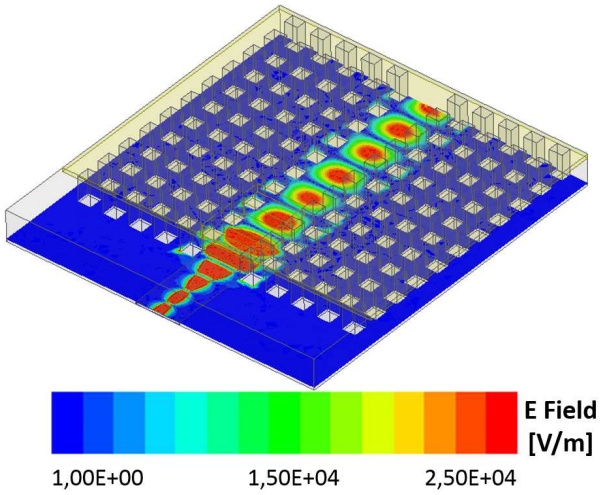

Fig. 8: E-Field distribution of the microstrip to GGW transition at 92.5 GHz.

smaller than the nominal value, the transition behavior remains hardly unaffected. The performance gets worse at the central frequency but in any case the reflection coefficient is below -18 dB. However, when the air gap increases, there is a certain degradation of the performance and the bandwidth below -15 dB is reduced. Nonetheless, the performance is still acceptable and represents a good solution for H-plane splits.

In addition, different errors related to misalignments of the microstrip substrate have been considered. First, the misalignment in the waveguide longitudinal direction, i.e. z direction according to Fig. **??** has been analysed. In this case the misalignment produces the microstrip taper length to be shorter than designed and the substrate enters into the second Chebyshev transformer step, see the inset in Fig. **??** for clarification.

The simulation results for different values of misalignment are shown in Fig. **??**. The response is still acceptable for 100 μm, with $S_{11} \leq -12\ dB$ for almost the whole band. However, for 500 μm the performance is not satisfactory. This degradation is produced by two effects: on the one hand the microstrip taper line becomes shorter than required and its final impedance is different from the impedance of the DFGGW; on the other one, the dielectric enters the second step and modifies its impedance and wavelength. Both effects modify the response of the Chebyshev adapter.

Another effect that has been taken into account is the misalignment in the transverse direction, i.e. in the x direction according to Fig. **??**. This positioning error implies that the pins touch the dielectric substrate and therefore the air gap at their end becomes equal to the substrate thickness, i.e. 0.127 mm. Therefore, the nominal case corresponds to the substrate centred with the GGW, but with this value of h, different from the optimum, 80 μm. In this case, the effect is more important than in the previous one, see Fig. **??**, mainly because, due to the loss of symmetry, the displacement prevents the microstrip taper line to excite properly the GGW mode. As a matter of fact, a high order resonance is excited for misalignments larger than 30 μm. Nonetheless, the performance is still acceptable until the displacement is 100 μm. Thus, the alignment pins in the microstrip substrate are necessary in order to guarantee accurate assembly.

Finally, the effect that the substrate has a cutting error so

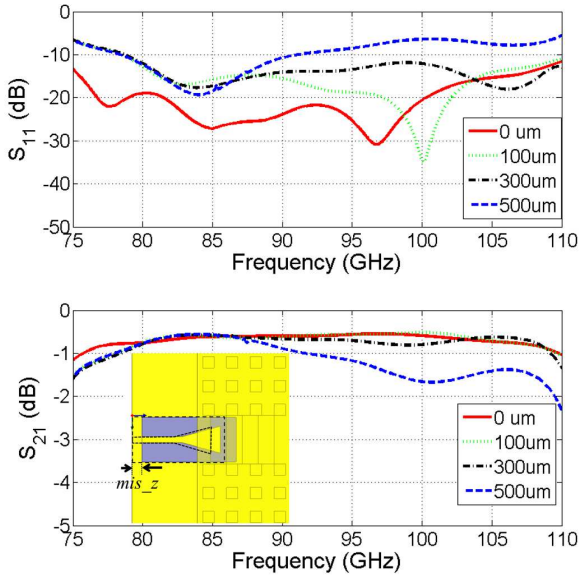

Fig. 10: Evaluation of the effect on the misalignment of the microstrip substrate in the z direction, given by different values of mis_z. The inset shows the displaced microstrip substrate and its nominal position (in dashed line).

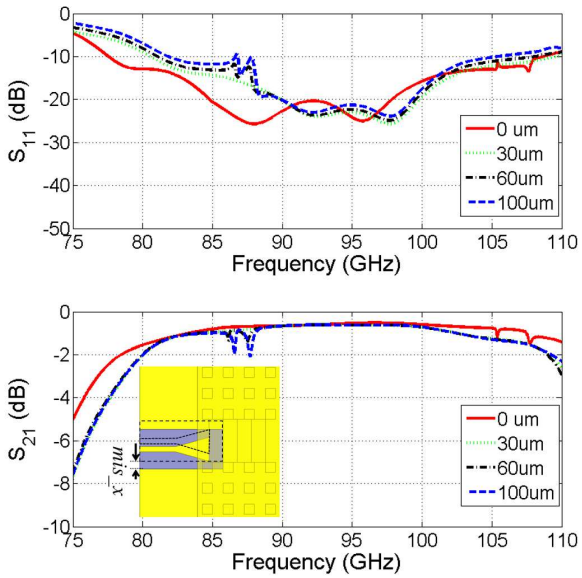

Fig. 11: Evaluation of the effect on the misalignment of the microstrip substrate in the x direction, given by different values of mis_z. The inset shows the displaced microstrip substrate and its nominal position (in dashed line). The nominal case corresponds to $h = 127$ μm.

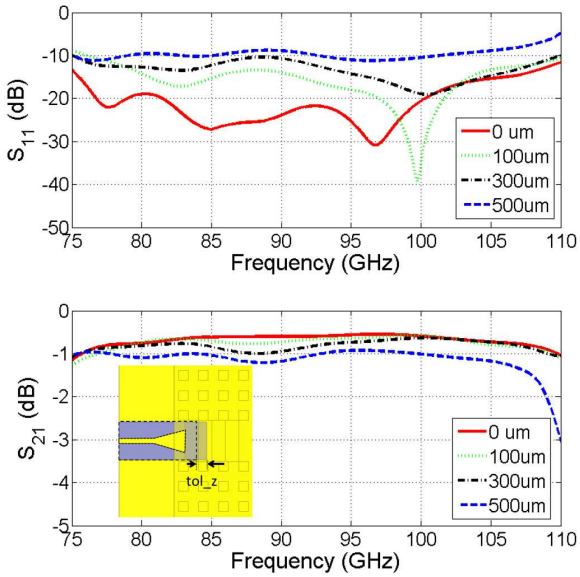

Fig. 12: Evaluation of the effect on the substrate length, given by different values of tol_z. The inset shows the microstrip substrate and its nominal dimensions (in dashed line).

that it is longer than the designed one has been evaluated . The effect is shown in Fig. **??**. This error is not so critical, since it just affects the impedance and propagation constant of the second transformer section. The S11 is below -10 dB for all cases; thus the circuit is tolerant to this misalignment.

III. Manufacturing and Experimental validation

In order to verify the transition performance, the back-to-back configuration was manufactured and tested. As explained previously, the two transitions were separated by a 5.18 mm long microsrip line. The behaviour of the whole structure is not affected by this microstip length; however, the longer the microstrip the higher the circuit global losses. The GGWs were 9 mm long and were connected directly to the WR10 rectangular waveguides of the W-band millimetre wave extenders.

The metallic block was micromachined in aluminium and split in the H-Plane. The pins are machined just in one of the metallic blocks, the other one being flat. Proper alignment was guaranteed by eight screws and eight alignment pins. Since a tight contact between the upper and bottom metallic parts is not required, the manufacturing tolerances can be relaxed.

The microstrip transition was manufactured by a standard photolithography procedure at the Public University of Navarra's facilities. First, the bare substrate is cleaned, and afterwards coated with a 7 μm layer of AZ nlof 2070 negative photoresist. The photoresist is baked at 110^o and exposed to ultraviolet light. After exposing, the photoresist is developed with the AZ726 chemical developer. The photoresist that has not been exposed to UV light is removed and then the substrate is metallized with 2 μm of copper. Finally, a technical stripper, NI555, is applied to the substrate, removing the metallized photoresist. The final step consists on cutting the circuit with

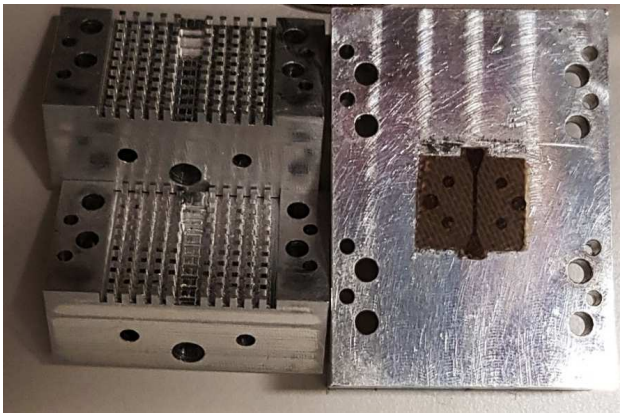

(a)

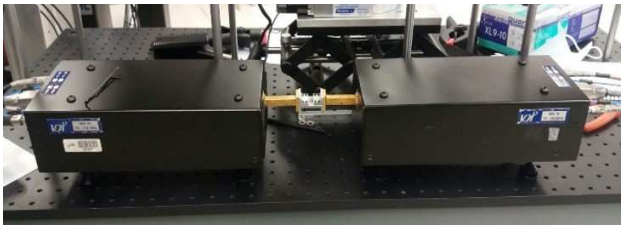

(b)

Fig. 13: Photographs of the fabricated prototype and measurement set-up. (a) Microstrip line printed on Rogers CuClad 233 substrate on the bottom metallic block and the two bed of pins. (b) Back-to-back transition connected to the VDI W-Band extenders.

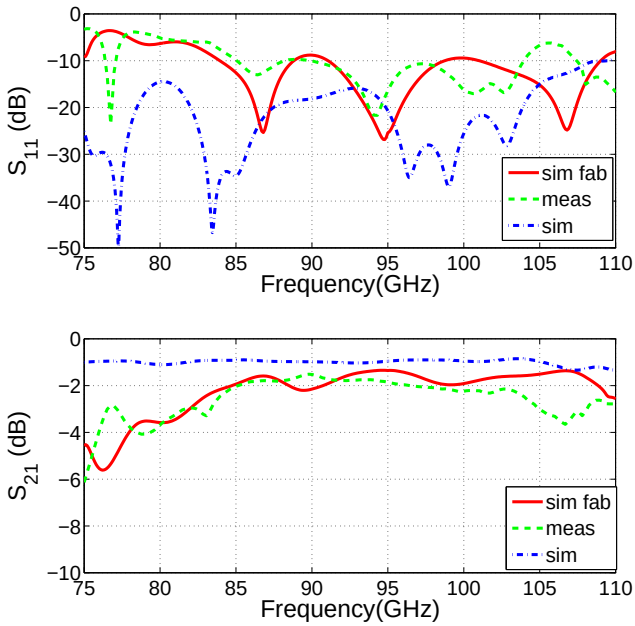

Fig. 14: Comparison between the predicted performance (point dashed line), the simulation taking into account fabrication errors (solid line) and measurement results (dashed line) of the back-to-back transition.

the required shape. For this purpose, a LPKF ProtMatH100 milling machine was been used. Photographs of the fabricated prototype can be seen in Fig. **????**.

The circuit assembly is simple. The substrate is placed in the bottom metallic block with the help of the alignment pins. It is then tightly screwed and finally the circuit is closed with the top metallic block. It is not necessary to weld or glue any part.

Once assembled, the back-to-back transition was measured with an Agilent PNA-X E3861 Microwave Network Analyser with two VDI W-Band VNA Extenders. Previously the equipment was calibrated using the standard TRL (Through, Reflect, Line) calibration kit. Fig. **????** shows a photograph of the measurement setup. A comparison between the measurements and the back-to-back simulation, for the ideal case and for the case taking into account the deviation of the dimensions produced by the tolerance error in the fabrication process is plotted in Fig. **??**. These dimensions have been measured with a Mitutoyo Hyper MF-U 176-402-43 measuring microscope.

Comparing with the simulation results, shown with point-dash line, where manufacturing errors are not taken into account, the cut-off frequency and the response is blueshifted and there is certain degradation in terms of performance. The frequency shift is ascribed to the narrower manufactured GGW channel, which is 2.39 mm wide instead of 2.45 mm. Nonetheless, the predicted response, once the fabricated values are introduced in the simulation model, is in good agreement with the measured performance. The best measured insertion loss is 1.5 dB at 90.4 GHz, with 3 dB mean value if the full W-band is considered. In addition, in the 85 - 105 GHz band the insertion loss is better than 2 dB. These losses include those in the transition and in the microstrip line. For the 5.18 mm long microstrip line the losses computed by HFSS are 0.66 dB. If the transition is considered symmetric and the losses of the microstrip line are removed, the transition losses can be estimated as 1.17 dB for each single transition, i.e. the taper and the Chebyshev transformer. Finally, the return loss is better than 10 dB from 83.9 GHz to 109 GHz, except for a resonant peak at 105 GHz.

IV. Conclusion

An inline microstrip to groove gap waveguide transition which allows for analytic design has been presented in this paper. This solution provides a good alternative for MMIC packaging and connection to GGW components. In order to prove this concept, a W-band transition based on the back-to-back configuration has been validated, presenting good agreement with the simulations: return loss better than 10 dB and insertion loss lower than 2 dB.

Acknowledgment

The authors would like to thank financial support by the Spanish MINECO, Project No. TEC2013-47753-C3-1-R and Project No. TEC2016-76997-C3-1-R.

References

[1] B. Panzner, “In-band wireless backhaul for 5G millimeter wave cellular communications - interactive live demo” *2015 IEEE Conference on Computer Communications Workshops*, Hong Kong, 2015, pp. 21-22.

[2] J. Hasch, E. Topak, R. Schnabel, T. Zwick, R. Weigel and C. Waldschmidt, "Millimeter-Wave Technology for Automotive Radar Sensors in the 77 GHz Frequency Band," *IEEE Trans. Microw. Theory Tech.*, vol. 60, no. 3, pp. 845–860, March 2012.
[3] D. M. Sheen, D. L. McMakin and T. E. Hall, "Three-dimensional millimeter-wave imaging for concealed weapon detection," *IEEE Trans. Microw. Theory Tech.*, vol. 49, no. 9, pp. 1581–1592, Sep. 2001.
[4] T. A. Midford, J. J. Wooldridge, and R. L. Sturdivant, "The evolution of packages for monolithic microwave and millimeter-wave circuits," *IEEE Trans. Antennas Propag.*, vol. 43, no. 9, pp. 983—991, Sep. 1995.
[5] E. Rajo-Iglesias and P.-S. Kildal, "Numerical studies of bandwidth of parallel plate cut-off realized by bed of nails, corrugations and mushroom-type EBG for use in gap waveguides," *IET Microw. Antennas Propagat.*, vol. 5, no. 3, pp. 282-–289, Mar. 2011.
[6] E. Rajo-Iglesias, A. U. Zaman, and P.-S. Kildal, "Parallel plate cavity mode suppression in microstrip circuit packages using a lid of nails," *IEEE Microw. Wireless Compon. Lett.*, vol. 20, no. 1, pp. 31-–33, Jan. 2010.
[7] E. Rajo-Iglesias, E. Pucci, A. A. Kishk, and P.-S. Kildal, "Suppression of parallel plate modes in low frequency microstrip circuit packages using lid of printed zigzag wires," *IEEE Microw. Wireless Compon. Lett.*, vol. 23, no. 7, pp. 359-–361, Jul. 2013.
[8] A. U. Zaman, M. Alexanderson, T. Vukusic, and P.-S. Kildal, "Gap waveguide PMC packaging for improved isolation of circuit components in high-frequency microwave modules," *IEEE Trans. Compon. Packag. Manuf. Technol.*, vol. 4, no. 1, pp. 16—25, Jan. 2014.
[9] A. Rebollo, R. Gonzalo, and I. Ederra, "Optimization of a Pin Surface as a Solution to Suppress Cavity Modes in a Packaged W-band Microstrip Receiver," *IEEE Trans. Compon. Packag. Manuf. Technol.*, vol. 4, no. 6, pp. 975–982, Jun. 2014
[10] Y. Shi, M. Zhou, and J. Zhang, "Parallel plate mode suppression in low frequency microwave circuit packages using lid of 3-D cross by a 3-D printing technique," *IEEE Trans. Electromagn. Compat.*, vol. 59, no. 4, pp. 1268—1271, Aug. 2017.
[11] P. S. Kildal, "Three metamaterial-based gap waveguides between parallel metal plates for mm/submm waves," *2009 3rd European Conference on Antennas and Propagation*, Berlin, 2009, pp. 28–32.
[12] P. S. Kildal, E. Alfonso, A. Valero-Nogueira and E. Rajo-Iglesias, "Local Metamaterial-Based Waveguides in Gaps Between Parallel Metal Plates," *IEEE Antennas Wireless Propag. Lett.*, vol. 8, pp. 84–87, 2009.
[13] A. Berenguer, V. Fusco, D. E. Zelenchuk, D. Sánchez-Escuderos, M. Baquero-Escudero, and V. E. Boria-Esbert, "Propagation characteristics of groove gap waveguide below and above cutoff," *IEEE Trans. Microw. Theory Techn.*, vol. 64, no. 1, pp. 27-–36, Jan. 2016.
[14] A. U. Zaman, P.-S. Kildal, and A. A. Kishk, "Narrow-band microwave filter using high-Q groove gap waveguide resonators with manufacturing flexibility and no sidewalls," *IEEE Trans. Compon. Packag., Manuf. Technol.*, vol. 2, no. 11, pp. 1882-–1889, Nov. 2012.
[15] A. Vosoogh, A. A. Brazález, and P.-S. Kildal, "A V-band inverted microstrip gap waveguide end-coupled bandpass filter," *IEEE Microw. Wireless Compon. Lett.*, vol. 26, no. 4, pp. 261—263, Apr. 2016.
[16] A. Farahbakhsh, D. Zarifi, and A. U. Zaman, "60-GHz groove gap waveguide based wideband H-plane power dividers and transitions: For use in high-gain slot array antenna," *IEEE Trans. Microw. Theory Techn.*, vol. 65, no. 11, pp. 4111-–4121, Nov. 2017.
[17] B. Ahmadi and A. Banai, "Substrateless amplifier module realized by ridge gap waveguide technology for millimeter-wave applications," *IEEE Trans. Microw. Theory Techn.*, vol. 64, no. 11, pp. 3623—3630, Nov. 2016.
[18] U. Nandi, A. U. Zaman, A. Vosoogh and J. Yang, "Novel Millimeter Wave Transition From Microstrip Line to Groove Gap Waveguide for MMIC Packaging and Antenna Integration," *IEEE Microw. Wireless Comp. Lett.*, vol. 27, no. 8, pp. 691–693, Aug. 2017.
[19] Y. Zhou, H. Liu, E. Li, G. Guo and T. Yang, "Design of a wideband transition from double-ridge waveguide to microstrip line," *2010 International Conference on Microwave and Millimeter Wave Technology*, Chengdu, 2010, pp. 737–740.
[20] A. Algaba Brazález, J. Flygare, J. Yang, V. Vassilev, M. Baquero-Escudero and P. Kildal, "Design of F-Band Transition From Microstrip to Ridge Gap Waveguide Including Monte Carlo Assembly Tolerance Analysis," *IEEE Trans. Microw. Theory Tech.,* vol. 64, no. 4, pp. 1245-1254, April 2016.
[21] Y. Shi, J. Zhang, S. Zeng and M. Zhou, "Novel W-band Millimeter Wave Transition From Microstrip Line to Groove Gap Waveguide for MMIC Integration and Antenna Application," *IEEE Trans. Antennas Propag.*, vol. 66, no. 6, pp. 3172–3176, jun. 2018.
[22] Y. Zhang, J. A. Ruiz-Cruz, K. A. Zaki and A. J. Piloto, "A Waveguide to Microstrip Inline Transition With Very Simple Modular Assembly," *IEEE Microw. Wireless Comp. Lett.*, vol. 20, no. 9, pp. 480-482, Sept. 2010.
[23] A. Rebollo, R. Gonzalo and I. Ederra, "An Inline Microstrip-to-Waveguide Transition Operating in the Full W-Band", *J. Infrared Millim. Terahertz Waves*, Vol. 36, pp. 734-744, 2015.
[24] J. M. Pérez-Escudero, A.E. Torres-García, R. Gonzalo and I. Ederra, "A Simplified Design Inline Microstrip-to-Waveguide Transition", *Electronics,* vol. 7, no 10, pp. 215, 2018.
[25] D. M. Pozar, "Microwave engineering", 4^{th} *ed., John Wiley & Sons,* 2011.
[26] S. J. Orfanidis, "Electromagnetic Waves and Antennas", NJ, Piscataway, Online Book., Aug. 2016, [online] Available: http://www.ece.rutgers.edu/ orfanidi/ewa/.
[27] I. A. Eshrah, A. A. Kishk, A. B. Yakovlev and A. W. Glisson, "Rectangular waveguide with dielectric-filled corrugations supporting backward waves," *IEEE Trans. Microw. Theory Tech.*, vol. 53, no. 11, pp. 3298-3304, Nov. 2005.

Jose M. Pérez-Escudero was born in Murcia, Spain, in 1988. He received the Degree in Telecommunication Engineering from the Universidad Politécnica de Cartagena, Murcia, Spain.

From September of 2013 to March of 2014 he was with Fraunhofer Institute for High Frequency Physics and Radar Techniques FHR, Bonn, Germany, where he was working on waveguide and planar technology filters and their applications in Radar systems. Since April 2015 he is with the Antenna Group at the Electrical, Electronic and Communication Department of the Public University of Navarra as Predoctoral Research Fellow.

His interests include Terahertz components, antennas and their applications in the millimeter and sub-millimeter wave ranges.

Alicia E. Torres-García was born in Cuba in 1990. She received the Degree in Telecommunication Engineering from the Instituto Superior Politécnico José Antonio Echeverría (ISPJAE), Havana, Cuba, in 2013.

She is currently working as a Predoctoral Research Fellow in the Antenna Group in the Electrical, Electronic and Communication Engineering Department of the Public University of Navarre (UPNA), Spain.

Her interests include millimeter wave and THz components and antennas, metamaterials, planar antennas and different research fields in the microwave range.

Ramón Gonzalo (M'94) received the M.Sc. and Ph.D. degrees (Hons.) in Ingeniero de Telecomunicación from the Public University of Navarra (UPNA), Pamplona, Spain.

Since 1995, he has been with the Antenna Group, Electrical and Electronic Engineering Department, UPNA, where he is currently a Full Professor. From 1997 to 1998, he was a Research Fellow of the Antenna Section, ESA-ESTEC, Noordwijk, The Netherlands. From 2008 to 2010, he was the Head of the Electrical and Electronic Engineering Department. He is a member of the Institute of Smart Cities, UPNA, Pamplona. He has authored over 60 journal publications in peer-reviewed magazines and 100 conference papers related to his research lines.

Dr. Gonzalo was a co-recipient of the LAPC 2006, LAPC 2007, and IWAT 2007 Best Paper Award.

Iñigo Ederra (M'2015) received the Ingeniero de Telecomunicación and Ph.D. degrees from the Universidad Pública de Navarra, Pamplona, Spain, in 1996 and 2004, respectively.

In 1997, he joined the Microwave and Millimetre Wave Group, Universidad Puública de Navarra. From 1999 to 2000 he was with the European Space Research and Technology Centre (ESTEC), ESA, Noordwijk, The Netherlands, where he was working on Electromagnetic Bandgap materials and their applications in the field of antennas. Since 2001 he is with the Antenna Group, Universidad Pública de Navarra. From June to October 2002 he was visitor scientist at the Rutherford Appleton Laboratory, Chilton, Didcot, UK, participating in ESA's Startiger I project. Currently, he holds an Associate Professor position at the Universidad Pública de Navarra and is a member of its Institute of Smart Cities.

His research interests are in the field of Metamaterials and Metasurfaces and their applications in microwave, millimetre wave and THz components and antennas.